Octave Spanning Tunable Frequency Comb from a Microresonator

P. Del'Haye,[1,2,3] T. Herr,[2] E. Gavartin,[2] M. L. Gorodetsky,[4] R. Holzwarth,[1,3] and T. J. Kippenberg[1,2,*]

[1]*Max-Planck-Institut für Quantenoptik, 85748 Garching, Germany*
[2]*École Polytechnique Fédérale de Lausanne (EPFL), 1015 Lausanne, Switzerland*
[3]*Menlo Systems GmbH, 82152 Martinsried, Germany*
[4]*Faculty of Physics, Moscow State University, Moscow 119991, Russia*

(Received 24 January 2011; published 1 August 2011)

We report the generation of an octave-spanning optical frequency comb in a continuous wave laser pumped microresonator. The generated comb spectrum covers the wavelength range from 990 to 2170 nm without relying on additional external broadening. Continuous tunability of the generated frequency comb over more than an entire free spectral range is demonstrated. Moreover, the linewidth of individual optical comb components and its relation to the pump laser phase noise is studied. The ability to derive octave-spanning spectra from microresonator comb generators represents a key step towards f-$2f$ self-referencing of microresonator-based optical frequency combs.

DOI: 10.1103/PhysRevLett.107.063901 PACS numbers: 42.65.Ky, 06.20.fb, 42.65.Hw, 42.82.Et

Optical frequency combs [1–4] enable precise measurements of optical frequencies and can be used in a wide range of scientific and technological applications. Recently, a new class of frequency comb generators has emerged [5–7], based on parametric frequency conversion of a continuous wave (CW) laser inside a high-Q silica microresonator [8]. In addition, this method has been demonstrated in a variety of other microresonator geometries and materials, including crystalline calcium fluoride resonators [9–11], fused silica microspheres [12], silicon nitride microresonators [13,14], as well as compact fiber cavities [15] and high index silica based microresonators [16]. However, to date no octave-spanning combs have been demonstrated utilizing microresonators, which are required to achieve self-referencing with an f-$2f$ interferometer.

Here, we present octave-spanning frequency comb generation in optical microresonators. Moreover, we demonstrate continuous tunability of the comb, providing a route to self-referencing [2–4] of high repetition rate microresonator-based frequency combs as required for metrology applications. The employed experimental setup is depicted in Fig. 1(a) and consists of an external cavity diode laser (ECDL) that is amplified by an erbium doped fiber amplifier (EDFA) to an output power of up to 2.5 W. The light is coupled into a microresonator mode using a tapered optical fiber [17]. Owing to the high power coupled into the resonator, the optical modes experience a significant thermal frequency shift, requiring a large (ca. 1 THz) tuning range of the laser to stay resonant with the cavity mode. The laser is tuned into a resonance from high to low frequencies, which results in thermal self-locking [18] of the microresonator mode to the pump laser. The optical frequency comb is monitored by two optical spectrum analyzers (OSA). Figure 1(b) shows that when pumping with 2.5 W of power at 1560 nm, a spectrum spanning more than one octave is directly generated inside the microresonator. This spectrum has been recorded using a 80 μm-diameter microresonator with a mode spacing of 850 GHz and a quality factor of $Q \approx 2.7 \times 10^8$.

An important prerequisite for many applications of an optical frequency comb is its tunability. Especially for spectroscopy with a frequency comb with large mode separation, it is advantageous to be able to position a comb mode at any frequency of interest. While control and stabilization of mode spacing and offset frequency of a microresonator-based frequency comb have been shown in previous work [6], tunability of the pump laser frequency (defining one of the comb lines) over more than an entire free spectral range of the microresonator is presented here. This remarkable tuning capability is shown in Fig. 2. The thermal effect allows the microresonator modes to follow the pump laser frequency within a tuning range exceeding 1 THz, while an octave-spanning frequency comb from 140 to 280 THz is maintained over nearly 500 GHz tuning range. Since this frequency shift only depends on material properties of the microresonator, namely, the thermal expansion, thermally induced refractive index change and the optical Kerr effect, it is possible to derive the temperature change of the resonator material. For this calculation the contribution of the Kerr effect is subtracted first, being responsible for an estimated resonance shift of $\Delta\nu_{\mathrm{Kerr}} \approx 100$ GHz. The Kerr shift is estimated using $\Delta\nu_{\mathrm{Kerr}} \approx \frac{n_2}{n_0^2}\frac{cQP_{\mathrm{in}}}{4\pi^2 R A_{\mathrm{eff}}}$ for a microresonator with a radius of $R = 40$ μm, an optical quality factor of $Q \approx 2 \times 10^8$, an effective mode area of $A_{\mathrm{eff}} \approx 4$ $\mu\mathrm{m}^2$, a launched power of $P_{\mathrm{in}} \approx 1$ W, the speed of light in vacuum c and the linear ($n_0 = 1.44$) and nonlinear ($n_2 = 2.2 \times 10^{-20}$ $\frac{\mathrm{m}^2}{\mathrm{W}}$) refractive index of fused silica. Subtracting the Kerr contribution leads to a thermally induced mode shift of $\Delta\nu_{\mathrm{therm}} \approx 900$ GHz. This equates to a temperature change of $\Delta T = \frac{\Delta\nu_{\mathrm{therm}}}{\alpha\cdot\nu} \approx 800$ K (with $\alpha = 6 \times 10^{-6}$ K^{-1} being a combined constant describing both

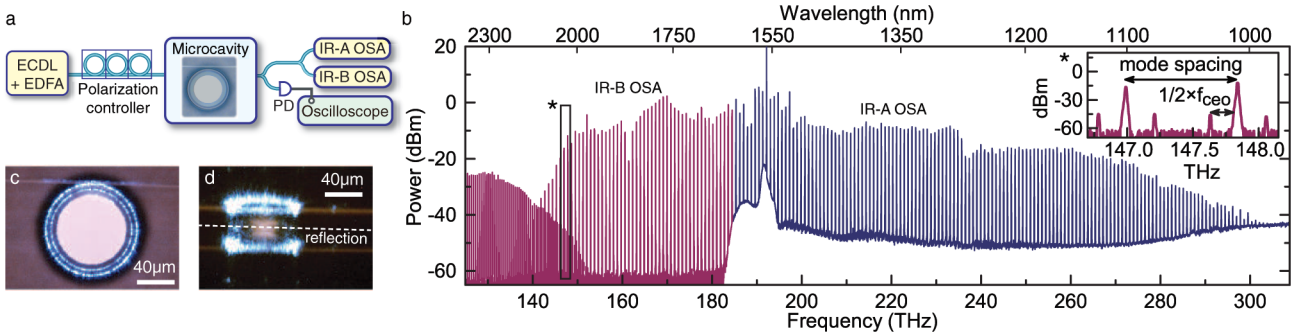

FIG. 1 (color online). Octave-spanning frequency comb generation in a microresonator. (a) Experimental setup with external cavity diode laser (ECDL), erbium doped fiber amplifier (EDFA), photo diode (PD), and optical spectrum analyzers (IR-A OSA, 0.6–1.7 μm; IR-B OSA, 1.2–2.4 μm). (b) Octave-spanning optical frequency comb, generated in a 40 μm-radius microresonator with a mode spacing of 850 GHz. The denser lines on the low frequency side are a replica of the high frequency end of the spectrum at half the frequency due to the grating spectrometer's second order diffraction. This artifact allows us to determine the carrier envelope offset frequency from the optical spectrum within the resolution of the spectrum analyzer (inset). (c),(d) Microscope images of the fused silica microresonator. The 1 μm light can be detected by the CMOS camera.

the thermal expansion and thermally induced refractive index change of fused silica). However, the temperature change is still well below the annealing point at 1140 °C and the softening point at 1665 °C of fused silica. On first notice, Fig. 2 appears to show a uniform comb shift with the pump laser frequency, corresponding to a pure carrier envelope offset frequency change. However, closer inspection reveals a slight variation of the comb spacing as a result of a change in intracavity power due to changed detuning between pump laser and microcavity mode [6]. Figure 3 shows the variation of the mode spacing and the carrier envelope offset frequency based on the data in Fig. 2. The influence of the pump laser detuning on the mode spacing is rather small with 4.83 GHz/THz compared to the impact on the carrier envelope offset frequency, which equates to 153 GHz/THz.

The geometry of a microresonator is critical for broadband comb generation. Mode profile and resonance frequencies of different microresonator geometries were simulated using finite element methods [19], taking geometrical and material dispersion into account (Fig. 4). The geometries are defined by a fixed microresonator radius of 40 μm and a set of different minor radii (cross sections). Based on these simulations the resonator's group delay dispersion (GDD) and the resulting wavelength dependent mismatch $\Delta\nu$ between positions of the equidistant comb modes and resonator modes (which are not equidistant due to dispersion) can be derived [20]. The simulations show that the extent of the minor radius—which is experimentally controllable—considerably influences mismatch and dispersion of the resonator. However, even for a dispersion optimized geometry the mismatch in the wings of octave-spanning combs exceeds 10 GHz [Fig. 4(d)]. An explanation for the broadband comb generation is cross- and self-phase modulation induced frequency pulling similar to processes in mode locked lasers [21,22]. In contrast to earlier work [5], the ability to generate octave-spanning combs is mainly attributed to optimized resonator dispersion as well as higher optical quality factors and higher pump power. While a flat dispersion is beneficial for broad comb generation and microresonator modes, this has to be balanced with the increasing mode area, raising the power threshold [23] for the four-wave mixing process. A dispersion optimized resonator geometry with a radius of

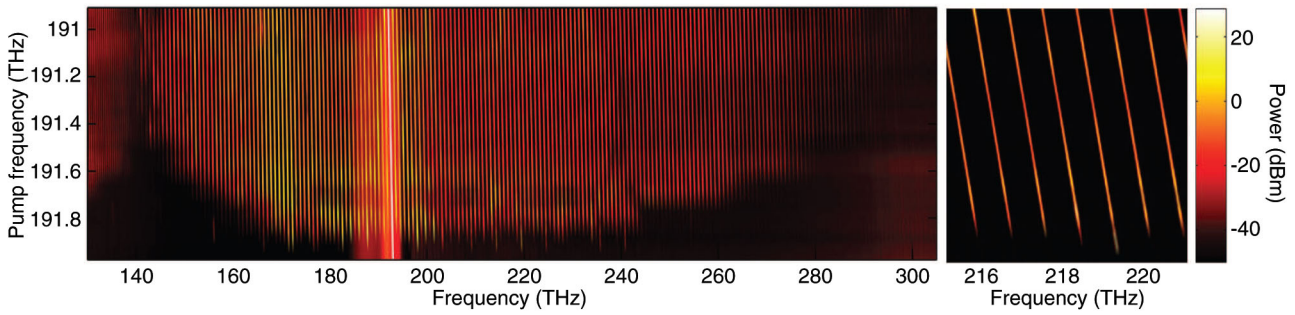

FIG. 2 (color online). Tunable octave-spanning microresonator-based frequency comb. The horizontal axis shows the measured frequency comb at different pump laser frequencies (vertical axis). The brightest line corresponds to the pump laser (with a power of 1 W in this measurement). A magnified part of the spectrum in the right panel shows that the comb lines can be tuned more than a full free spectral range.

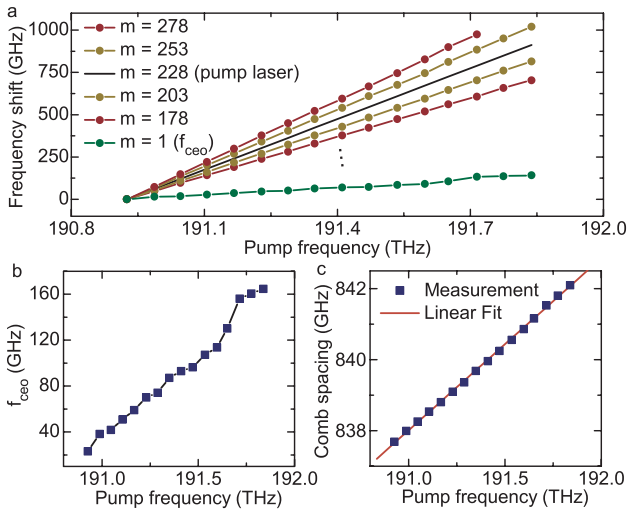

FIG. 3 (color online). Microresonator comb tuning parameters. (a) Measured frequency shift of the ± 25th and ± 50th sideband with respect to the pump laser at different pump laser detuning (m denotes the mode number of the comb line). The black line has a slope of 1 and reflects the shift of the pump laser itself. The line with $m = 1$ shows the shift of the carrier envelope offset frequency f_{ceo}. (b),(c) Effect of the pump frequency detuning on f_{ceo} and comb spacing.

40 μm and a cross section radius of 2.8 μm is used for the experiments.

An important property of the generated comb modes is their linewidth. A fiber laser ($\lambda = 1050$ nm, <50 kHz short term linewidth) is employed to record a beat note with the high frequency end of the comb (Fig. 5). The observed linewidth corresponds to $\Delta f \approx 70$ MHz, which is significantly broader than the noise observed in more narrow combs [5,6] and exceeds the cold cavity linewidth (~ 1 MHz). Further measurements reveal that the pump laser noise imprints itself also on modes that are not participating in the FWM process, i.e., it leads to cavity frequency noise of the optical resonator. The width of the measured beat note exhibits a complex dependence on both pump power and detuning of the laser with respect to the cavity resonance. Figures 5(d) and 5(f) show that changes in the pump laser detuning can strongly influence the comb linewidth. In addition, under certain coupling conditions we observed not a single beat note but multiple beat notes. One possible origin of this splitting can be due to mechanical modes of the resonator, which are coupled via radiation pressure (which has been extensively studied in both silica [24] and crystalline [25] microresonators). Another possible origin of this phenomenon can be merging of subcombs generated at different wavelengths with different repetition rates. Indeed, the linewidth of microresonator as well as comb modes is influenced by different noise processes, including thermorefractive noise, thermoelastic noise, thermal Brownian motion, ponderomotive noise, photothermal noise, and self- and cross-phase modulation noise [26,27]. Self- and cross-phase modulation is estimated to be the major contributor to the observed linewidth, which is given by the single sided noise spectral density

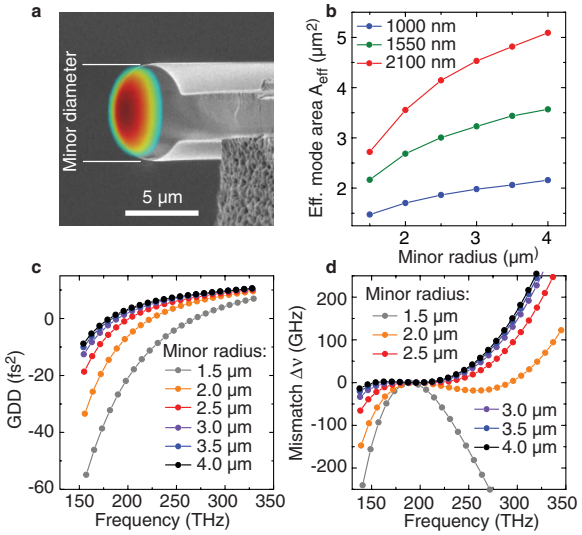

FIG. 4 (color online). Simulation of mode area and dispersion. (a) Simulated mode profile superimposed on a scanning electron microscope image of a cleaved microresonator. (b) Simulated effective mode area for different wavelengths. (c),(d) Simulated group delay dispersion (GDD) and mismatch $\Delta\nu$ between positions of equidistant comb modes and resonator modes (for zero mismatch at the pump laser frequency of 193 THz). The larger radii show a reduced influence on the resonator dispersion (traces for 3.5 and 4 μm radius are nearly identical).

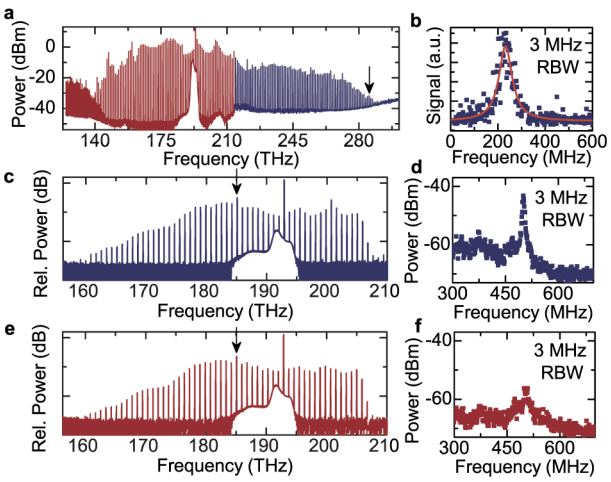

FIG. 5 (color online). Linewidth of frequency comb modes. (a),(b) Octave-spanning comb with pump laser at 1550 nm and corresponding radio frequency beat note with a fiber laser at 1050 nm (arrow in spectrum). (c),(d) Comb in different resonator with narrowband beat note (measured with 3 MHz resolution bandwidth). Comb and beat note in (e),(f) show the transition to a broader beat note at different detunings between pump laser and microresonator resonance. The beat notes in (d),(f) are generated with an additional external cavity diode laser at the positions of the arrows in the spectra in (c),(e).

$$S_{\nu\nu}^{\mathrm{comb}}(\Omega) = \left(\frac{\nu}{n_0}\right)^2 \frac{(2n_2)^2}{A_{\mathrm{eff}}^2} S_{PP}^{\mathrm{cav}}(\Omega), \quad (1)$$

where $S_{PP}^{\mathrm{cav}}(\Omega)$ denotes the spectrum of fluctuations of the intracavity power. Diode lasers generally exhibit substantial excess phase noise [28] and we experimentally determine the noise of the employed diode laser $S_{\phi\phi}^{\mathrm{pump}}$ to be approximately 80–100 dB above the quantum level $S_{\phi\phi}^{\mathrm{quant}} = h\nu/P_{\mathrm{in}}$ for a pump power of $P_{\mathrm{in}} = 2$ W and Fourier frequencies Ω from dc to well above the cavity cutoff given by $\kappa/2\pi \approx 10$ MHz. This phase noise is in a critically coupled high-Q cavity most efficiently converted to intracavity amplitude noise via quadrature rotation

$$S_{PP}^{\mathrm{cav}}(\Omega)|_{\Delta=\kappa/2} = 4\bar{P}_{\mathrm{pump}}^2 \frac{\Omega^2/\tau_{\mathrm{rt}}^2}{\kappa^4 + 4\Omega^4} S_{\phi\phi}^{\mathrm{pump}}(\Omega), \quad (2)$$

for a laser-cavity detuning of $\Delta = \kappa/2$ and where τ_{rt} denotes the cavity round trip. Inserting this expression into Eq. (1) and integrating according to

$$\delta\nu_{\mathrm{rms}} = \left[2\int_{\Omega^*}^{\infty} S_{\nu\nu}(\Omega)\frac{d\Omega}{2\pi}\right]^{1/2} \quad (3)$$

allows estimating a resulting comb linewidth of $\delta\nu_{\mathrm{rms}} \approx 4$ GHz. This shows that the amount of linewidth broadening induced by the pump laser phase noise can significantly exceed the cold cavity linewidth explaining the striking observation in Fig. 5(f) (beat note broader than $\kappa/2\pi$). The lower integration boundary $\Omega^*/2\pi = 1$ MHz in Eq. (3) denotes the inverse measurement time. For smaller detuning this noise decreases and is finally governed by the much smaller pump laser amplitude fluctuations. However, operating the comb too close to zero detuning does not allow for a stable thermal self-lock [18]. Importantly, for a quantum limited pump laser of 2 W the linewidth would equate to approximately $\delta\nu_{\mathrm{rms}} =$ 200 kHz, indicating that significant improvements may be possible using a low phase noise pump laser.

The ability to generate a full octave-spanning frequency comb within a monolithic microresonator is a further step towards direct integration of optical frequency standards into compact microphotonic devices. Microresonator-based combs can complement conventional combs sources in applications where high repetition rate, high power per comb line, tunability, and bandwidth is critical, such as astrophysical spectrometer calibration [29], optical arbitrary waveform generation [30], direct comb spectroscopy [31], advanced telecommunications, microwave frequency generation [9], or optical coherence tomography [32].

This work was funded by a Marie Curie IAPP, the Swiss National Science Foundation, the NCCR for Quantum Photonics, and the DFG funded Nanosystems Initiative Munich (NIM). M. L. Gorodetksy acknowledges support of the Dynasty Foundation. Experimental work was conducted by P. D. and T. H.

*tobias.kippenberg@epfl.ch

[1] R. Holzwarth *et al.*, Phys. Rev. Lett. **85**, 2264 (2000).
[2] D. J. Jones *et al.*, Science **288**, 635 (2000).
[3] T. Udem, R. Holzwarth, and T. W. Hänsch, Nature (London) **416**, 233 (2002).
[4] S. T. Cundiff and J. Ye, Rev. Mod. Phys. **75**, 325 (2003).
[5] P. Del'Haye *et al.*, Nature (London) **450**, 1214 (2007).
[6] P. Del'Haye *et al.*, Phys. Rev. Lett. **101**, 053903 (2008).
[7] T. J. Kippenberg, R. Holzwarth, and S. A. Diddams, Science **332**, 555 (2011).
[8] Y. K. Chembo, D. V. Strekalov, and N. Yu, Phys. Rev. Lett. **104**, 103902 (2010).
[9] A. A. Savchenkov *et al.*, Phys. Rev. Lett. **101**, 093902 (2008).
[10] I. S. Grudinin, N. Yu, and L. Maleki, Opt. Lett. **34**, 878 (2009).
[11] A. A. Savchenkov *et al.*, Nat. Photon. **5**, 293 (2011).
[12] I. H. Agha *et al.*, Phys. Rev. A **76**, 043837 (2007).
[13] J. S. Levy *et al.*, Nat. Photon. **4**, 37 (2009).
[14] M. Foster *et al.*, arXiv:1102.0326.
[15] D. Braje, L. Hollberg, and S. Diddams, Phys. Rev. Lett. **102**, 193902 (2009).
[16] L. Razzari *et al.*, Nat. Photon. **4**, 41 (2009).
[17] J. C. Knight *et al.*, Opt. Lett. **22**, 1129 (1997).
[18] T. Carmon, L. Yang, and K. J. Vahala, Opt. Express **12**, 4742 (2004).
[19] M. Oxborrow, IEEE Trans. Microwave Theory Tech. **55**, 1209 (2007).
[20] P. Del'Haye *et al.*, Nat. Photon. **3**, 529 (2009).
[21] H. A. Haus and A. Mecozzi, IEEE J. Quantum Electron. **29**, 983 (1993).
[22] C. R. Menyuk *et al.*, Opt. Express **15**, 6677 (2007).
[23] T. J. Kippenberg, S. M. Spillane, and K. J. Vahala, Phys. Rev. Lett. **93**, 083904 (2004).
[24] T. J. Kippenberg, H. Rokhsari, T. Carmon, A. Scherer, and K. J. Vahala, Phys. Rev. Lett. **95**, 033901 (2005).
[25] J. Hofer, A. Schliesser, and T. J. Kippenberg, Phys. Rev. A **82**, 031804 (2010).
[26] A. E. Fomin *et al.*, J. Opt. Soc. Am. B **22**, 459 (2005).
[27] A. B. Matsko *et al.*, J. Opt. Soc. Am. B **24**, 1324 (2007).
[28] T. C. Zhang *et al.*, Quantum Semiclass. Opt. **7**, 601 (1995).
[29] T. Steinmetz *et al.*, Science **321**, 1335 (2008).
[30] F. Ferdous *et al.*, arXiv:1103.2330.
[31] S. A. Diddams, L. Hollberg, and V. Mbele, Nature (London) **445**, 627 (2007).
[32] D. Huang *et al.*, Science **254**, 1178 (1991).